Emission rate assessment of airborne brake particles by characterization of the pad and disc surfaces from a pin-on-disc tribometer

Florian Philippe, Maiqi Xiang, Martin Morgeneyer, Yan-Ming Chen, Pierre Charles, Frédéric Guingand, Christophe Bressot

Original Article

Toxicology Research and Application

Toxicology Research and Application
Volume 4: 1–9

DOI: 10.1177/2397847320977782
journals.sagepub.com/home/tor
SAGE

Emission rate assessment of airborne brake particles by characterization of the pad and disc surfaces from a pin-on-disc tribometer

Florian Philippe[1,2], Maiqi Xiang[1], Martin Morgeneyer[1], Yan-Ming Chen[3], Pierre Charles[2], Frédéric Guingand[2] and Christophe Bressot[4]

Abstract

Particles from brake, road and tire wear contribute to about half of the emissions (PM10) of particulate traffic pollution. It is estimated that 50 to 70% of the brake debris material is transformed into an emission of polydisperse aerosols. In order to improve the understanding of the brake debris generation and its dependency on the brake material, the wear of a disc and a brake pad from a standard production car were studied. The disc was made of perlitic cast iron with lamellar graphite and subjected to standard braking cycles. Microscopic evaluation was performed on the disc track, as well as analyses by Energy Dispersive Spectroscopy (EDS). Finally, a metallographic section has been made in the longitudinal direction of friction to better understand the morphology. The study focuses on disc surface oxidation and morphology of a thin layer on both disc and pin surface. Particle concentrations increase with the friction power and the area of contact surface. The observations show that the generation of particles can be the result of the oxidation of the disc surface during friction by two- and three-body abrasion when braking.

Keywords

Emission risk assessment, airborne brake particles, pin-on-disc, characterization of the pad and disc surfaces, tribometer, brake emission

Date received: 16 September 2020; accepted: 9 November 2020

Introduction

Particles from brake, road and tire wear contributes to about half of the emissions (PM10) of particulate traffic pollution.[1] The specific contribution of brake wear particles remains undetermined, but it is estimated that 50 to 70% of the debris material is transformed into an emission of polydisperse aerosols[2] while the contribution of braking may become predominant due to the expected reduction of engine emissions, *i.e.* by changing the engine type from combustion to electric motors.

In a report of 2019, the European Environment Agency estimated that PM2.5 exposure was accountable of 412 000 premature deaths in 41 European countries.[3] Those premature deaths are also seen as a total of 4 223 000 years of life lost.[3] The toxicity of braking emissions remains unclear. It is however known that majority of braking particles fits in PM2.5 category.[4]

[1] University of Technology of Compiègne, Centre Pierre Guillaumat, TIMR Department, Compiègne, France
[2] Groupe PSA, DRIA Department, Route de Gisy, Vélizy-Villacoublay, France
[3] CETIM, MMS Department, Senlis, France
[4] INERIS, Verneuil-en-Halatte, France

Corresponding author:
Florian Philippe, University of Technology of Compiègne, Centre Pierre Guillaumat, 60200 Compiègne, France; Groupe PSA, Route de Gisy, 78140 Vélizy-Villacoublay, France.
Emails: florian.philippe@utc.fr; florian.philippe@mpsa.com

The difference between data from literature highlights the need to better document the subject through reliable, standardized and transdisciplinary methodologies.[5,6] The measurement of braking particles in real-life situations results in cross-contamination, but a confined test bench might help to reach an experimental consensus on the subject.

The dynamometer is an instrument able to experimentally simulate the contact between brake pads and brake disc. This device is designed to experimentally replicate friction between braking materials. In a dynamometer, real-life braking equipment such as a brake pad and a disc are used. For this reason, the majority of researchers study brake particles with a dynamometer bench.[5–8] In practice, a disc rotates with a defined inertia, representing the simulated vehicle mass. Two small plates come into contact with the disc to slow it down. This operation is close to that observed in a real car. Several parameters are controlled such as initial speed, final speed, initial rotor temperature, braking deceleration and the number of stops. It is possible to choose the rotation speed of the disc, the inertia of the disc, the pressure of the pads and the braking time. By this, all parameters of the "Worldwide Harmonized Light Vehicles Test Procedure" (WLTP) cycle can be applied.[9]

Another approach is to experimentally simulate braking friction using a mount with a disc and solely a disc pin, which is a classic piece of equipment for experimentally simulating friction contact between materials. This pin-on-disc bench is commonly used to determine the coefficient of friction, the quality of the lubricant or to characterize tribofilm formation.[10] Alemani et al.[11] published a study showing the evolution of emissivity according to the different friction parameters on a pin-on-disc bench. In this study, the speeds and pressures used are close to driving conditions in the city. To compensate for the low emissions expected, the authors carried out continuous sliding tests over 14 km.

The essential difference between the dynamometer and the pin-on-disc pin is the power dissipated during braking. On a dynamometer, all the energy dissipated is evacuated by the air flow, which thus often is required to be large. This high flow rate can perturb both aerosol particle distribution and flow stability, making measurements more difficult. Another drawback of the dynamometer is the pollution of the whole system by depositions from previous tests and by the emission of many dynamic joints of the system.

The main role of brake is to transform kinetic energy to heat by friction. During this transformation, brake pad and disc materials can worn by several procedures, abrasion, adhesion and tribo-chemical reactions with oxydation of disc.[12] The worn material is generally under particle form in different dimensions. Particles smaller than 10 μm like PM10 and PM2,5 became often airborne particle.[13] The main tribological mechanism observed in this study is abrasive wear. In a discussion about two- and three-body abrasion, JD Gates[14] describes abrasive wear as "wear in which hard asperities on one body moving across a softer body under some load, penetrate and remove material from the surface of the softer body, leaving a groove". The such called hard asperities may be on a large material, in which case, the abrasive wear is of two-body abrasion nature. Hard asperities may also be small discrete particles resulting in three-body abrasion.[12]

When two surfaces are rubbed against each other a transfer of atoms happens.[15] Braking contacts are often performed in dry sliding conditions which enhance the material transfer phenomena. Those conditions may then result in the formation of transfer layers on the sliding surfaces. The transfer layer mediates the interaction of the two surfaces during sliding. The tribological properties at the sliding interface can also be changed by the presence of the transfer layer.[15]

This study thus focuses on pin-on-disc bench systems and its objective is to present optimized test conditions such as contact pressure, sliding speed, air flow and sampling parameters to provide a more sensitive and less expensive set up than the dynamometer for pre-selection testing of pad and disc materials. This study aims to improve the understanding of mechanisms of wear that generate aerosol particles and furthermore help to find solutions to reduce emissions.

Experimentation

Pin-on-disc tribometer

The pin-on-disc studied is a tribometer designed and manufactured by CETIM initially to investigate the friction of dry compressors segment/jacket parts.[16] It has been used in wear tests such as machine wires for textile and automotive and railway brakes.[17,18]

The rotation of the disc is driven by an electric motor fixed on a block with dampers. This block is independent of the assembly on which the pin is attached, which avoids the transmission of the engine vibrations on the pin-on-disc contact part. The transmission of torque is achieved by a belt woven and impregnated with elastomer that does not allow the vibrations to pass at high frequencies. The spindle is supported by two sloping roller bearings for high stiffness and low friction. Loading is carried out by a system of masses like many tribometers of this type. The particularity is that the load is applied horizontally via a pulley and a parallelogram made of very thin steel blades, which allows application **of** very low loads (Figure 1). Another advantage of the horizontal system is the possibility to modify the mass of the support without changing the applied load, which is very interesting for the study of vibration and noise generated by friction. It is thus possible to control the loading speed, duration and number of cycles. The load can be set to a value ranging from 1 to 30 Newton (N). The machine is installed in a room where humidity is regulated by a steam generation system.

The pin-on-disc tribometer is placed in a confinement chamber to minimize disturbances due to particles already present in the air (air pollution and electric motor emissions). The new air of the confinement chamber is

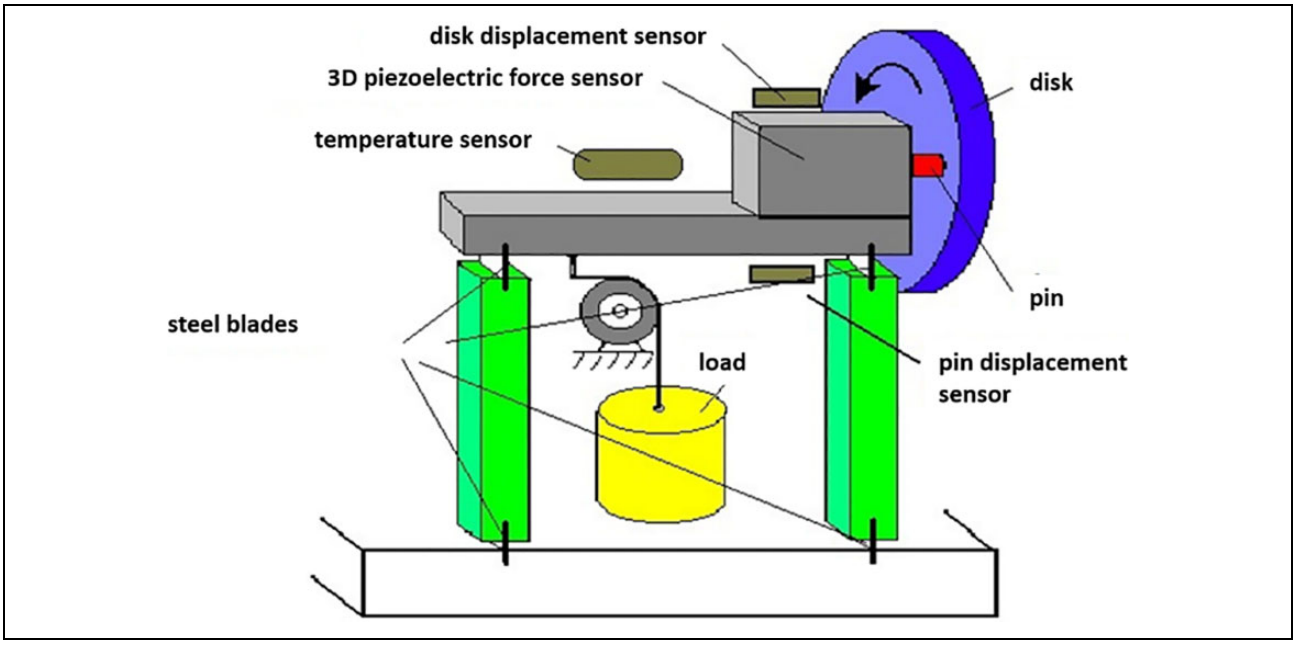

Figure 1. Design of the CETIM pin-on-disc.[16]

constantly filtered. The filtered air flow is constant during the test. The disc is a ventilated disc model with improved heat dissipation. In order to reduce ventilation disturbances, the confinement chamber, the air flow and the slight overpressure in the chamber is designed to optimize the detection of emission during the tests.

Methods for particle measurements

The two apparatus types used in this study for measuring aerosol particles are the Condensation Nucleus Counter (CNC),[19] and the Electrical Low Pressure Impactor (ELPI).[20]

Condensation Nucleus Counters (CNCs) are commonly used to measure the number of submicronic concentrations in air particles with sizes up to a few nanometers.[19,21] They are used in many applications, including ambient air, quality monitoring, workplace exposure measurements, laboratory testing, filtration efficiency or as a particle counter coupled to a Differential Mobility Analyzer (DMA) in a SMPS type particle detector.[22]

The ELPI is used to select particles by inertia and then electrically detect them.[6,12,23] The charged particles before their introduction into the device (corona charger) are then taken according to their size in an impactor where each stage has an electrical counting system. The ELPI provides a classification into 13 particle sizes with cut-off diameters of 7 nm to 10 µm. Due to their inertia, the larger objects accumulate on the upper levels, while the smaller ones are positioned on the lower levels. Each stage is equipped with an electrical system that delivers a signal that is dependent on the electrical load received. A size distribution is thus obtained with the number of classes corresponding to the number of stages in the impactor.

Table 1. List of the performed tests.

Pin diameter (mm)	Sliding speed (m/s)	Contact pressure (MPa)
4.65	13.9	0.43
4.65	13.9	0.65
4.65	13.9	1.24
4.65	13.9	1.83
4.65	25.0	0.43
4.65	25.0	0.65
4.65	25.0	1.24
4.65	25.0	1.83
4.65	36.1	0.43
4.65	36.1	1.24
4.65	36.1	1.83
10.0	13.9	0.43
10.0	25.0	0.43
10.0	36.1	0.43

The influence of friction power was also studied according to the 13 values in Table 1 over a total of 66 tests. Friction power defines the power dissipated during friction. It is described by the following equation (1):

$$P = \mu NSV \quad (1)$$

with P, the friction power (W), μ, the coefficient of friction (U.S.), N, the normal force applied (N), and V, the sliding speed (m/s).

Materials tested

The disc and brake pad are from a standard production car. The disc is made of perlitic cast iron with lamellar graphite.

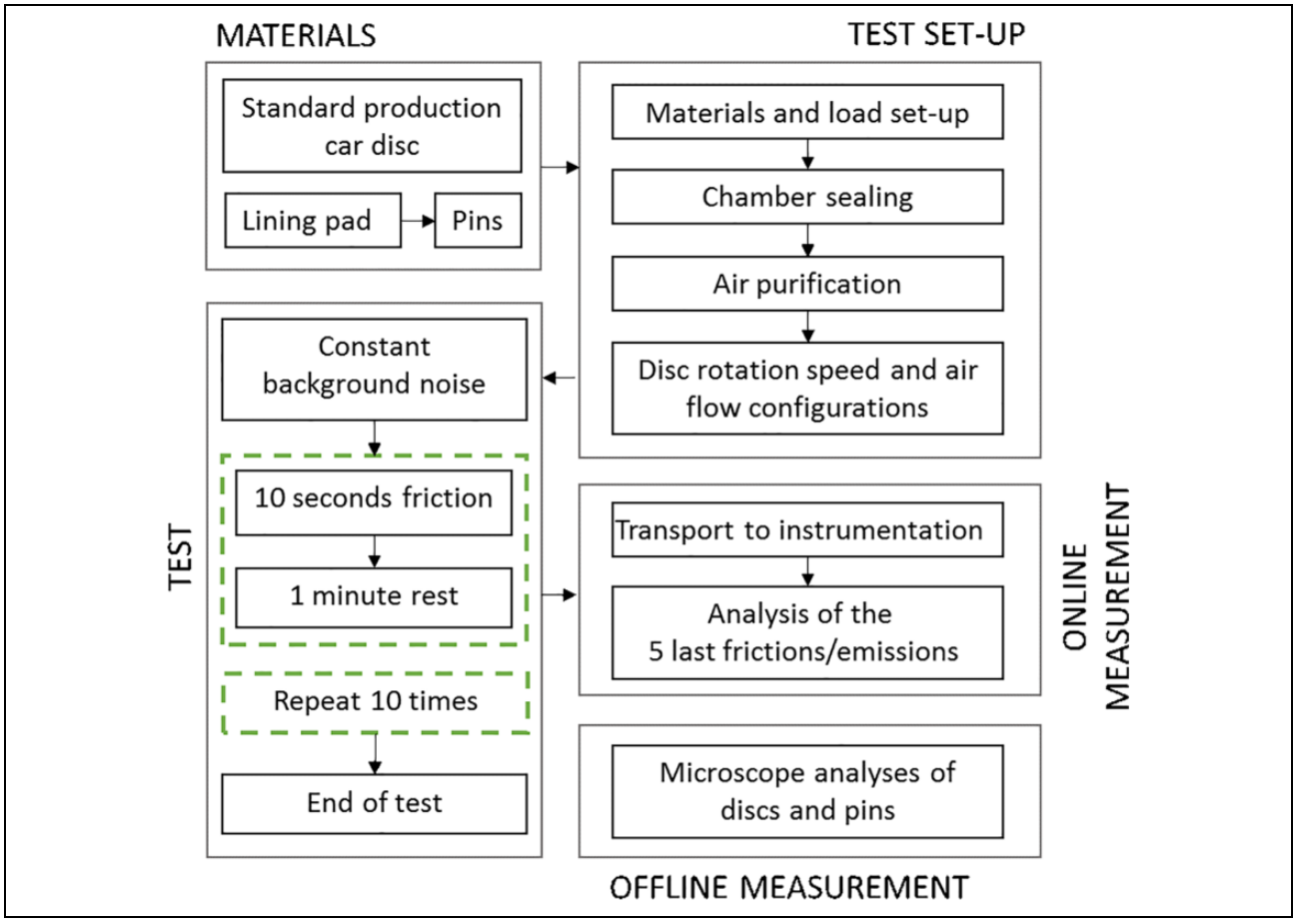

Figure 2. Flow diagram of the testing process.

This kind of cast iron is widely used on European market as it grants friction stability with graphite flakes. A coating is applied and can limit oxidation when storing the discs. The discs are ground with a series of beak-in friction tests during 30 frictions of 10 seconds at 25 m/s and under 1.24 MPa to remove this coating layer.

Lining pads can be divided in four categories: Non-Asbestos Organic (NAO), Semi-Metallic (SM), Low-Metallic (LM) and Ceramic pads. The pin is cut from a very common pad material in Europe (LM). Pads are consisted of at least seven components in four categories[12]:

- Binding materials sticks all components together and ensure thermal stability of the matrix.
- Reinforced fibers are used to improve friction performance and strength.
- Fillers are used to reduce the cost of friction material and to improve processability.
- Reinforcing fibers[12,24,25] are added in pad to control wear rates of both pad and disc and to ensure stable frictional properties.[12,24] Abrasive particles increase coefficient of friction and give better defined rubbing surface by removing iron oxides and other undesired surface films from the disc.[12,24]

These components are usually associated with about 20 chemical elements. The specifications of the brake linings vary greatly from one vehicle to another. This variability gives rise to a multitude of formulations needed for braking efficiency.

The pins are taken by high pressure water jet cutting to avoid any thermal damage during machining. Two sizes of pins were used in this study: 4.65 mm and 10.0 mm in diameter to have larger variation of contact pressure.

Test conditions

Figure 2 is a flow diagram of the testing process used. Preparing tests needed to purify air of the pin-on-disc chamber. When background noise is steady and low enough to ensure good test sensibility, test starts. In order to mimic actual driving conditions, four contact pressures and three sliding speeds were used in this study (Table 1).[9] The particle emission is defined here as the average of the sum of the particles emitted during the last five friction tests.

To have a similar initial condition, each test series is preceded by a 10-second run-in at 25 m/s and 1.24 MPa. Each test consists of 10 contact sequences at constant contact pressure and sliding speed. Each contact sequence lasts

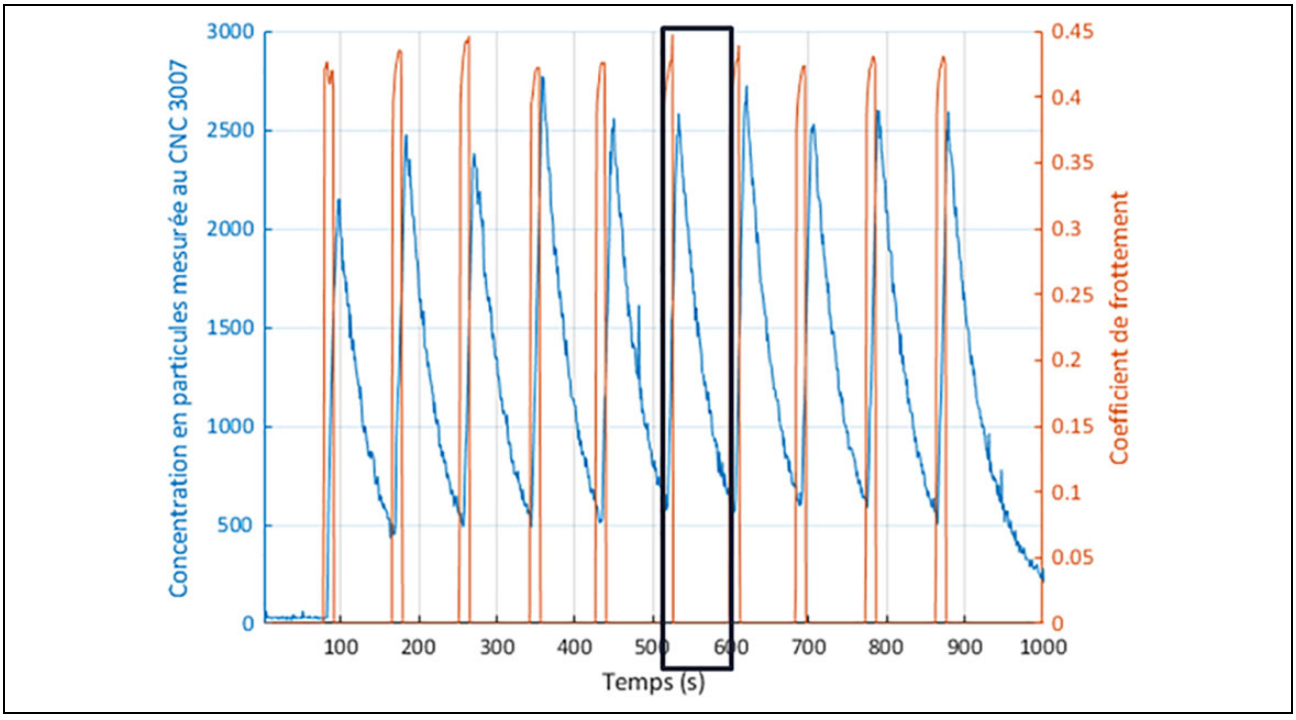

Figure 3. Coefficient of friction and concentration measured by CNC during a test at 1.24 MPa and 25.0 m/s (PV = 31 MPa.m/s).

10 seconds with 1 minute of rest between the sequences. This minute of intervening time is planned to make possible a return to particle concentrations close to the initial background noise counting.

Results of the tests

Figure 3 shows an example of the concentration measured at CNC 3007 and the coefficient of friction while a speed of 25 m/s and a pressure of 1.24 MPa on a 4.65 mm diameter pin are applied. The friction coefficient curve (red curve) highlights the stable value between 0.4 and 0.45 during the braking period. The particle concentration curve (blue curve) stabilizes around 10 #/cm^3 at the starting point of the test, suggesting the low level of particles entering the containment chamber after filtration. The peaks can reach 2750 #/cm^3 during the friction between the pin and the disc. Ten contact sequences were performed as shown in the μ curve, and 10 peaks of particle concentrations are observed during the test. In addition, peak concentrations always appear after the increase in the measured friction coefficient.

Between two contact sequences, particle concentration goes down rapidly but did not return to the baseline. Thus, from the second friction, each emission is impacted by the previous emission. These residual concentrations from the previous test can be up to 650 #/cm^3. These residual concentrations can be significantly reduced by increasing the time between frictions.

The black rectangle highlights the analysis area defined for each emission. Thus, the data between the beginning and the end of the emission are processed electronically under MATLAB. The different concentrations in the range are summed and corrected by ambient noise. In the plotted example, the total emission of the interval is 6.3×10^4 #/cm^3 and the average over the last five friction events is equal to 6.5×10^4 #/cm^3. Tests with identical conditions were carried out just after tests at different conditions in order to investigate the influence of the initial condition of the pin surface and the friction track of the disc.

Series of tests have been performed with different test conditions than previously *i.e.* speed and pressure, in order to investigate the influence of the initial condition of the pin surface and the friction track of the disc. Emission levels are assessed for the different initial configurations. It is observed that the number of particle emitted increases with friction power.

In order to understand particle generation mechanisms, microscopic evaluations were performed on disc track. The disc track after a test at 0.43 MPa and 13.9 m/s (PV = 5.8 MPa.m/s) observed on an optical microscope equipped with a dynamic focusing device is illustrated by Figure 4. The surface is partially covered with gray areas that were not observed on the initial material. Most of those areas have an elongated shape following the friction direction. Analyses by EDS (Energy Dispersive Spectroscopy) were carried out on a friction runway to determine the nature of these gray areas. This analysis shows that these gray areas are enriched in oxygen compared to the mostly clear areas of iron. A

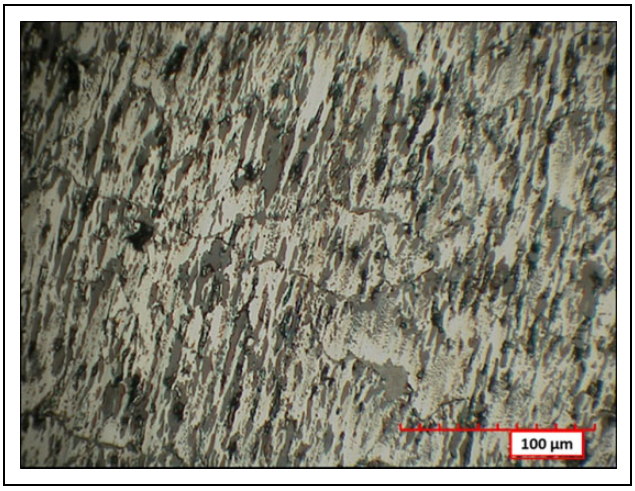

Figure 4. Disc track observed on optical microscopy when testing at 0.43 MPa of pressure and 13.9 m/s of speed (PV = 5.8 MPa.m/s).

Figure 5. Disc track observed on optical microscopy when testing at 1.24 MPa of pressure and 25.0 m/s of speed (PV = 31 MPa.m/s).

metallographic section was made in the longitudinal direction of friction to better understand the morphology of the gray zone. A homogeneous structure of lamellar graphite cast iron has been observed. The gray areas observed on the surface are poorly visible in sections, due to their small thickness (< 1 µm). Figure 4 also shows some abrasion strips. Lines can be also observed as cracks in network.

Figure 5 shows another example of a friction track after testing at 1.24 MPa and 25.0 m/s (PV = 31 MPa.m/s). Compared to the previous track, the gray area is significantly larger. An image analysis of these two photos indicates that the gray area represents 30% +/− 10% of the total area for the 5.8 MPa.m/s test, while it is 60% +/− 10% for the 31 MPa.m/s test. Abrasion stripes on this track appear to be greater than those on the track in Figure 4. Network lines are also observed on this runway.

Figure 6 shows a detailed observation of the surface of the disc after friction at 31 MPa.m/s at the SEM (Scanning Electron Microscope). Some of these gray areas appear to originate from surface material. The size fluctuations of the relief are about a few micrometers to several tens of micrometers. Other gray areas correspond to a change of color without formation of relief. Cavities of a few micrometers were found on the surface.

Figure 7 shows the pin surface when testing at 0.43 MPa and 13.9 m/s analyzed with optical microscopy. Friction surface appears to be heterogeneous. This surface is made of light-colored grains and dark colored grains. The shiny appearance of the pin surface is a clue suggesting a thin transfer layer. Real friction areas are distinguished by low-angled light photo which identifies upper plane surfaces. Image analysis was performed with image analysis software to determine the ratio of real friction surface/total surface. An extended analysis of the surface showed that real friction areas represent 20 ± 5% of the total pin surface. In a similar approach,

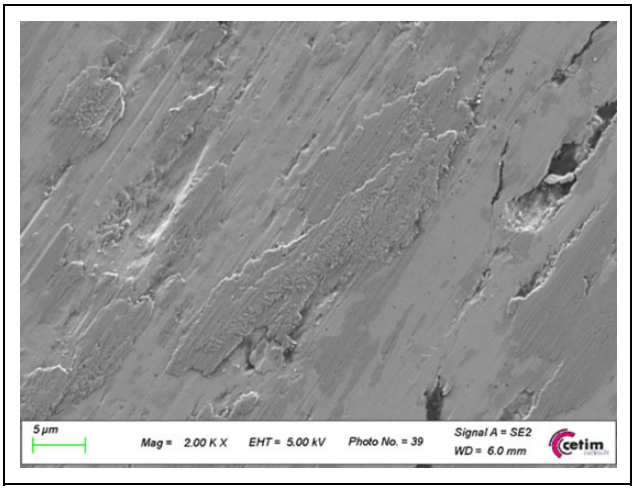

Figure 6. Disc SEM microscopy showing gray areas detailed when testing at 1.24 MPa of pressure and 25.0 m/s of speed (PV = 31 MPa.m/s).

Figure 8 reports the investigation of a pin surface when testing respectively with 1.24 MPa and 25.0 m/s as of speed and pressure during friction stress. Global analysis of this sample shows that 45 ± 5% of the pin is covered by real friction areas.

SEM and EDS analyses of the surface of a pin when testing with friction at 0.43 MPa of pressure and 13.9 m/s of speed (PV = 5.8 MPa.m/s) is presented in Figure 9. SEM analysis shows deep streaks can on the weakly conductive material (bottom of the image). The conductive material at the top center of the image is smooth and does not show streaks. Furthermore, another conductive material with an elongated shape at the top left of the image shows traces of wear by streaks. EDS analysis allow us to determine several other points:

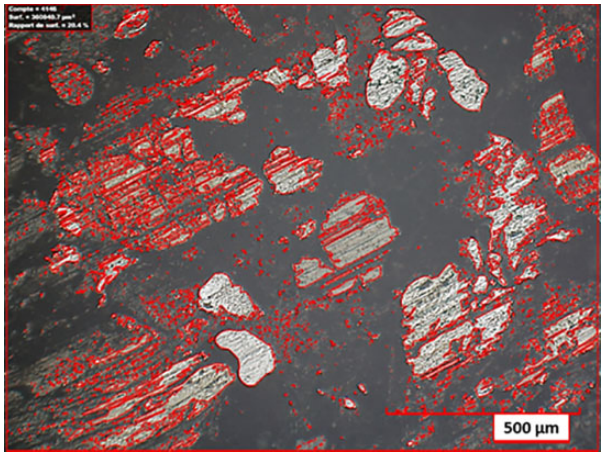

Figure 7. Optical microscopy of pin surface when testing at 0.43 MPa of pressure and 13.9 m/s of speed (PV = 5.8 m/s).

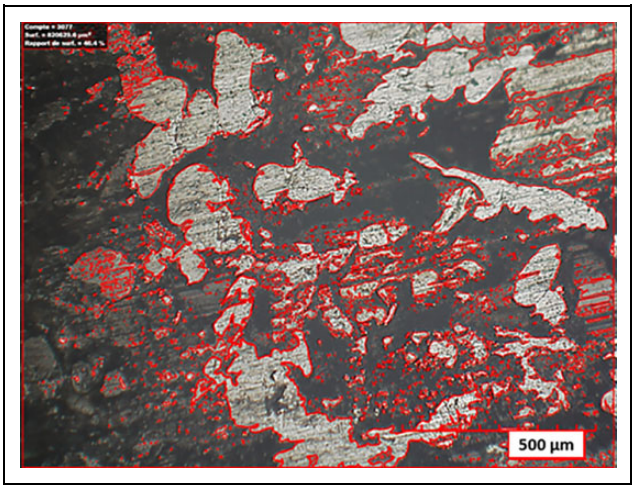

Figure 8. Optical microscopy of pin surface when testing at 1.24 MPa of pressure and 25.0 m/s of speed (PV = 31 m/s).

- Iron is observed here in two states. One is shown as worn objects with dimension of 40 µm × 120 µm. Those objects are mainly composed of iron and oxygen. The other iron material is observed as powder spread on most of the area.
- The poorly streaked material is mainly composed of silicone and zirconium.
- The material with strong streaks is rich in silicone, oxygen, magnesium and potassium.

Discussion

Two important questions should be discussed in this study, disc surface oxidation and morphology of thin layer on both disc and pin surface.

The EDS analysis showed that the gray areas on the disc friction track were enriched in oxygen compared with the original matrix. These gray areas correspond most likely to a disc surface that has been oxidized. Comparison between Figures 4 and 5 highlights a higher gray area surface when increasing the product PV (Pressure × Speed). So, the greater is the friction power, the greater will be the oxide layer. Similar observations were obtained by Riahi and Alpas[26] *i.e.* higher contact pressures and sliding speeds will drive to a larger proportion of the contact surface covered with oxide film. This increase in the coverage rate with the PV product could be explained by the increase in the contact temperature and consequently to a higher energy dissipated by the friction. The cast iron material of disc might be transformed to oxide at high temperature during braking action since the transformation is correlated to friction power.

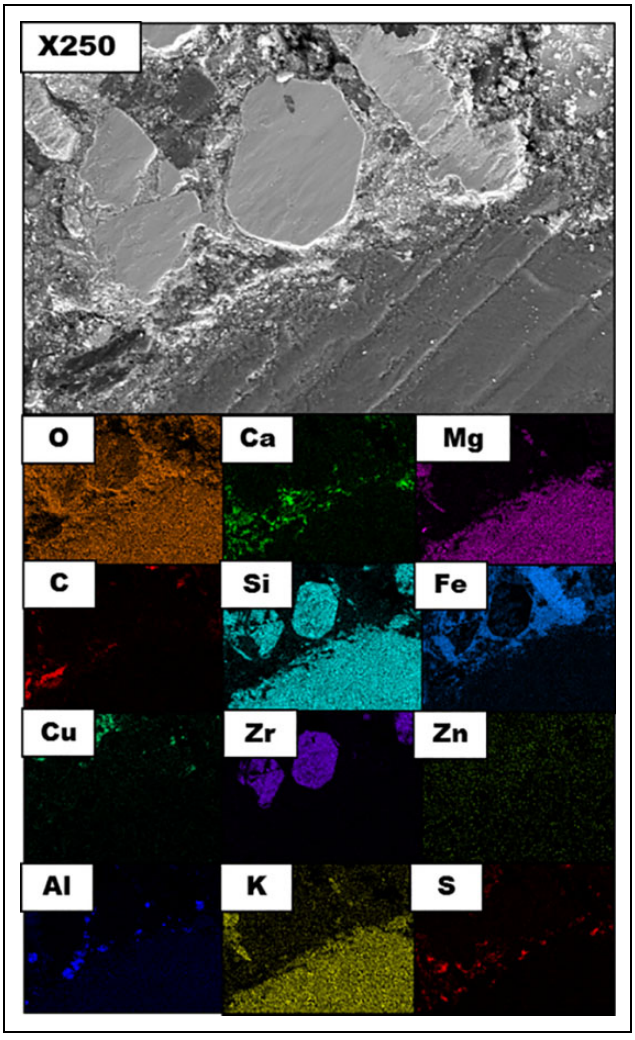

Figure 9. EDS analysis of a pin after a test at 0.43 MPa and 13.9 m/s (PV = 5.8 MPa.m/s).

To understand how the disc and pin material have been transformed to airborne particles, we are interested in the morphology of surface layer on both disc and pin surface. As shown in Figures 6 and 9 (SEM images), very thin reliefs on the wear track were observed on both pin and

disc surface. These reliefs could originate from supermicronic debris previously pulled out from the disc or pad and crushed onto the surface. The dimensions of the debris observed are also consistent with the size distributions measured at the ELPI assessing micrometric particle emissions. This transfer phenomenon was also noted by Riahi and Alpas[26] under a severe wear regimen. This tribological transferred layer (TTL) could be removed from both disc and pin surface to air by abrasion. Two-body and three-body abrasion may take place at the same time during braking. As observed in Figure 9, the presence of hard particles in the pad could cause two-body abrasion of disc by the high surface roughness to two bodies of the cast iron by the pad.

The presence of a thin layer of transfer on Figures 7 and 8 on the piece testifies to a three-body abrasion process of the cast iron by transfer layer on the contact plateaus of the pad.[24] The transfer layer observed on the pin could result from repetitive grinding of the wear debris, which would shrink as the cycles progressed. This gradual reduction in size of the debris could take place until the end of the friction, where the debris would then pull out from the tribological system to the air.

Iron oxides are more friable than metallic iron[12] and are therefore more able to be transformed into finer particles by successive grinding. The increase in emissivity with speed could therefore be caused by the greater coverage of the disc track by iron oxides, which would promote the successive crushing of debris. In addition, cracking lines and graphite pads can act as particle traps and keep them in contact longer. This could promote the process of transformation into small particles.

Conclusion

The braking tests were performed on a pin-on-disc tribometer supplemented with a chamber confined to the flow of filtered constant air before braking. The braking was carried out using a 4.65 and 10 mm diameter pin taken from classical materials like a commercial pad and a car brake disc.

The results of measurements using a Condensation Nucleus Counter show that the concentration of aerosol particles ranges from 7 to 1000 nm and can reach a peak of 2000 #/cm^3 during the 10 seconds of braking, while the level of particle concentration is about 20 #/cm^3 in the chamber before braking. Size distribution analysis by Electrical Low Pressure Impactor (ELPI) shows that maximum particle concentration is between 0.94 µm and 1.59 µm. CNC results showed that level of particle concentrations emitted increase with friction power. Microscopic observations show that oxidation of disc surface also tends to increase with friction power. The generation of particles can be the result of the oxidation of the disc surface during friction by two- and three-body abrasion during braking. Limiting abrasion mechanisms that occurs during braking could be a solution to reduce emission of braking particles.

Acknowledgements

Authors gratefully acknowledge our respective institutions for making this transdisciplinary project possible. Also, we acknowledge the financial support of the ANRT 2017/1023 in this project. The French Ministry for Ecology funding is gratefully acknowledged.

Declaration of conflicting interests

The author(s) declared no potential conflicts of interest with respect to the research, authorship, and/or publication of this article.

Funding

The author(s) received no financial support for the research, authorship, and/or publication of this article.

ORCID iD

Florian Philippe https://orcid.org/0000-0003-1990-4045

References

1. Guerreiro C, de Leeuw F, Foltescu V, et al. European environment agency. Air quality in Europe: 2015 report. [Internet]. Luxembourg: Publications Office; 2015. http://bookshop.europa.eu/uri?target=EUB:NOTICE:THAL15005:EN:HTML [accessed 4 November 2019].
2. Wahlström J and Olofsson U. A field study of airborne particle emissions from automotive disc brakes. *Proc Inst Mech Eng Part D: J Automob Eng* 2015; **229**(6): 747–757.
3. European Environment Agency. Air quality in Europe 2019—European Environment Agency [Internet]. https://www.eea.europa.eu//publications/air-quality-in-europe-2019 [accessed 9 October 2020].
4. Grigoratos T and Martini G. Brake wear particle emissions: a review. *Environ Sci Pollut Res* 2015; **22**(4): 2491–2504.
5. Hagino H, Oyama M and Sasaki S. Laboratory testing of airborne brake wear particle emissions using a dynamometer system under urban city driving cycles. *Atmos Environ* 2016; **131**: 269–278.
6. Perricone G, Alemani M, Metinöz I, et al. Towards the ranking of airborne particle emissions from car brakes—a system approach. *Proc Inst Mech Eng Part D: J Automob Eng* 2017; **231**(6): 781–797.
7. Iijima A, Sato K, Yano K, et al. Particle size and composition distribution analysis of automotive brake abrasion dusts for the evaluation of antimony sources of airborne particulate matter. *Atmos Environ* 2007; **41**(23): 4908–4919.
8. Kukutschová J, Moravec P, Tomášek V, et al. On airborne nano/micro-sized wear particles released from low-metallic automotive brakes. *Environ Pollut* 2011; **159**(4): 998–1006.
9. Mathissen M, Grochowicz J, Schmidt C, et al. A novel real-world braking cycle for studying brake wear particle emissions. *Wear* 2018; **414–415**: 219–226.

10. Österle W, Kloß H and Dmitriev AI. Friction control during automotive braking: experimental observations and simulation at nanometre scale. *Tribol—Mater Surf Interf* 2009; **3**(4): 196–202.
11. Alemani M, Wahlström J and Olofsson U. On the influence of car brake system parameters on particulate matter emissions. *Wear* 2018; **396–397**: 67–74.
12. Xiao X, Yin Y, Bao J, et al. Review on the friction and wear of brake materials. *Adv Mech Eng* 2016; **8**(5): 168781401664730.
13. Hagino H, Oyama M and Sasaki S. Airborne brake wear particle emission due to braking and accelerating. *Wear* 2015; **334–335**: 44–48.
14. Gates JD. Two-body and three-body abrasion: a critical discussion. *Wear* 1998; **214**(1): 139–146.
15. Cho MH, Cho KH, Kim SJ, et al. The role of transfer layers on friction characteristics in the sliding interface between friction materials against gray iron brake disks. *Tribol Lett* 2005; **20**(2): 101–108.
16. Chen Y-M, Richard C and de l'usure-Mesure T. Tribomètres et essais tribologiques. *Techniques de l'ingénieur Frottement et usure* 2011.
17. Ranganathan N (Mohan). *Materials characterization: modern methods and applications*. Boca Raton: CRC Press, 2016, p. 330.
18. Hentour K, Marsal A, Turq V, et al. Carbon nanotube/alumina and graphite/alumina composite coatings on stainless steel for tribological applications. *Mater Today Commun* 2016; **8**: 118–126.
19. The History of Condensation Nucleus Counters: Aerosol Science and Technology: Vol 33, No 4 [Internet]. https://www.tandfonline.com/doi/abs/10.1080/02786820050121512 [accessed 11 September 2020].
20. Marjamäki M, Keskinen J, Chen D-R, et al. Performance evaluation of the electrical low-pressure impactor (ELPI). *J Aerosol Sci* 2000; **31**(2): 249–261.
21. Keller A, Tritscher T and Burtscher H. Performance of water-based CPC 3788 for particles from a propane-flame soot-generator operated with rich fuel/air mixtures. *J Aerosol Sci* 2013; **60**: 67–72.
22. Kouam J, Songmene V, Djebara A, et al. Effect of friction testing of metals on particle emission. *J Mater Eng Perform* 2012; **21**(6): 965–972.
23. Sanders PG, Xu N, Dalka TM, et al. Airborne brake wear debris: size distributions, composition, and a comparison of dynamometer and vehicle tests. *Environ Sci Technol* 2003; **37**(18): 4060–4069.
24. Eriksson M, Bergman F and Jacobson S. On the nature of tribological contact in automotive brakes. *Wear* 2002; **252**(1): 26–36.
25. Chan D and Stachowiak GW. Review of automotive brake friction materials: Proceedings of the Institution of Mechanical Engineers, Part D: Journal of Automobile Engineering [Internet]. 9 août 2016. https://journals-sagepub-com.ezproxy.utc.fr/doi/10.1243/0954407041856773 [accessed 12 December 2019].
26. Riahi AR and Alpas AT. Wear map for grey cast iron. *Wear* 2003; **255**(1): 401–409.